

Review

Biochar-Derived Anode Materials for Lithium-Ion Batteries: A Review

Ntalane Sello Seroka ^{1,2,*}, Hongze Luo ²  and Lindiwe Khotseng ¹ ¹ Department of Chemistry, Faculty of Natural Sciences, University of the Western Cape, Robert Sobukwe Road, Private Bag X17, Bellville 7535, South Africa; lkhotseng@uwc.ac.za² Energy Centre, Smart Places Cluster, Council for Science and Industrial Research (CSIR), Pretoria 0001, South Africa; hluo@csir.co.za

* Correspondence: nseroka@csir.co.za

Abstract: Highly portable nanoelectronics and large-scale electronics rely on lithium-ion batteries (LIBs) as the most reliable energy storage technology. This method is thought to be both environmentally friendly and cost-effective. We provide a study of a low-cost, abundant, and renewable supply of carbon-based biomass with potential uses in LIBs. Renewable feedstocks have received significant attention in recent decades as promising tools for efficient and alternative anode materials for LIBs. Researchers can synthesise carbon-rich biochar through the pyrolytic process of biomass. Depending on the synthetic process, precise surface chemistry, and textural qualities such as specific surface area and porosity, this material can be customised to favour application-specific properties with a preferred application. In this research, we look at the performance of biochar in LIBs, its properties, and the biomass supply, and we discuss the prospects for these biomass-derived materials in energy storage devices.

Keywords: lithium-ion batteries; sugarcane bagasse; biochar; carbon; physicochemical properties

Citation: Seroka, N.S.; Luo, H.; Khotseng, L. Biochar-Derived Anode Materials for Lithium-Ion Batteries: A Review. *Batteries* **2024**, *10*, 144. <https://doi.org/10.3390/batteries10050144>

Academic Editor: Carolina Rosero-Navarro

Received: 18 February 2024

Revised: 22 March 2024

Accepted: 19 April 2024

Published: 24 April 2024



Copyright: © 2024 by the authors. Licensee MDPI, Basel, Switzerland. This article is an open access article distributed under the terms and conditions of the Creative Commons Attribution (CC BY) license (<https://creativecommons.org/licenses/by/4.0/>).

1. Introduction

Renewable energy is the most logical way to reduce global environmental issues. The development of renewable energy systems is very important, especially in developing energy storage systems that are not only efficient but also cost-friendly, making them easily accessible and affordable or, at best, reducing the cost of energy storage devices. Electrochemical energy storage systems (ESSs) like batteries are storage devices that store a lot of energy and complement the power densities they possess. The way in which performance can be further investigated is by cost, cyclability, storage, and gravimetric/volumetric energy density [1–4].

The use of electricity is unparalleled. In today's world, electrical energy contributes to about 12% of the energy being used by humans. The growing population and the scarcity of fossil fuels have caused an energy crisis and environmental problems. The main effect of this is pollution, as excess gas is released into the atmosphere. The release of gases such as nitrogen oxide and carbon monoxide can be very harmful to human health [5].

Nanoelectronics, such as energy storage devices, have gained a lot of attention because of their high-power densities. Lithium-ion batteries provide electrical endurance in automobiles. Lithium-ion batteries have great efficiency and performance, are lightweight, and have a large storage capacity. Lithium-ion batteries are secondary batteries, which means that they may be recharged and have a reversible response. To meet the demand for energy storage systems, an ideal material that is cost-effective, has improved electrochemical performance, and does not contribute to the ongoing global problem is desired [1,6].

Several carbonaceous nanomaterials, such as carbon nanofibers, nanotubes, and graphite, have been used as negative electrodes in lithium-ion batteries. Graphite has

shown advantages in terms of high capacity because of tailoring structural and morphologically defined preparations. However, graphite has its own drawbacks, including the need for sophisticated equipment to realise practical large-scale applications [7–9].

Thus, biomass is a renewable source rich in carbon material. They require facile synthesis of carbon from the pyrolysis of biomass. The physicochemical properties of this process enhance the properties of the amorphous carbon derived from biomass. The biomass could be pyrolyzed to produce biochar and used as a carbon substitute in the anode material. As a negative electrode, carbon-based biomass has seen a range of advantages in lithium-ion batteries, such as good cycling stability and high capacity. Moreover, lithium-ion batteries over the years have realised various structural material compositions. Over the years, the main objective has remained the same, which has always been to increase scalability while decreasing battery weight [10–12].

It is imperative to note that the overall functionality can be increased from the enhanced cyclability of the anode and the higher rate capabilities. To mention a few, the strategies include energy densities, long life span, and power. For example, nanostructured materials, such as anodes, and better cathode capacity, can improve electrode performance. Carbon has been known to be a very conductive material since the discovery of carbon black [13].

In this review study, we look at the porous structure of carbon generated from biomass and the role of textural features as negative electrode materials in LIBs, low-cost, abundant, and ecologically beneficial renewable sources derived from biomass waste. The evolution of biochar in LIBs has included anode materials and/or nanoadditives in carbon-free batteries. The pyrolysis temperature, doping processes, and their effects on Li-ion storage capacity, as well as other good electrochemical properties, are reviewed.

2. Synthesis Methods

The way a material is synthesised can affect how well the material will perform. There have been several synthesis methods that have been developed mainly based on pore size, particle structure, conductivity, and how simple the process is and its cost-efficiency, as shown in Figure 1. This section discusses some of the primary ways or ways in which biomass can be synthesised into biochar. Carbonaceous materials rely heavily on synthetic routes. For example, pyrolysis temperature, residence duration, reaction time, and environment all influence the final carbon material property. According to a previous study, increasing temperature reduces surface terminations such as volatile O and H concentrations as gases. Surface terminations play a significant role in the capacities and power densities because oxygen content drives lithium-ion deposition or insertion without the formation of dendrites. The pyrolytic temperature affects the oxygen content and/or new surface functionalities, and the porosity of the material changes depending on the amount of heat the material is exposed to [5,14–17].

The lattice oxygen can be oxidized to gaseous oxygen, causing irreversible reactions, and preventing Li from being released, resulting in lower initial Coulombic efficiency and poor rate performance. Researchers found that oxygen surface terminations (carboxylic acids, ketones, and lactones) resulted in reduced intrinsic electronic conductivity on mesoporous carbon anodes in sodium-ion batteries. However, oxygen functions such as carboxylic anhydrides and quinones enhanced the electronic conductivity, and notably, 20.12 wt% oxygen carboxyl-rich carbon had a high affinity for Na^+ and hence improved storage capacity in sodium-ion batteries [5,17].

Among the pyrolysis, activation, or thermochemical conversion of lignocellulosic biomass for biochar formation, torrefaction and hydrothermal carbonization techniques were used. These processes differ in their operating temperatures, with torrefaction regarded for this process in an inert environment under parameters such as air pressure and temperatures ranging from 200 to 300 °C. The synthetic technique is typically preferred for biofuel production. The most current technology involves a low-cost and environmentally beneficial route in which biochar is produced at extremely low temperatures (180–260 °C)

under increased water or steam pressures. Wet biomass does not need to be predried, making it suitable for waste streams [5,17].

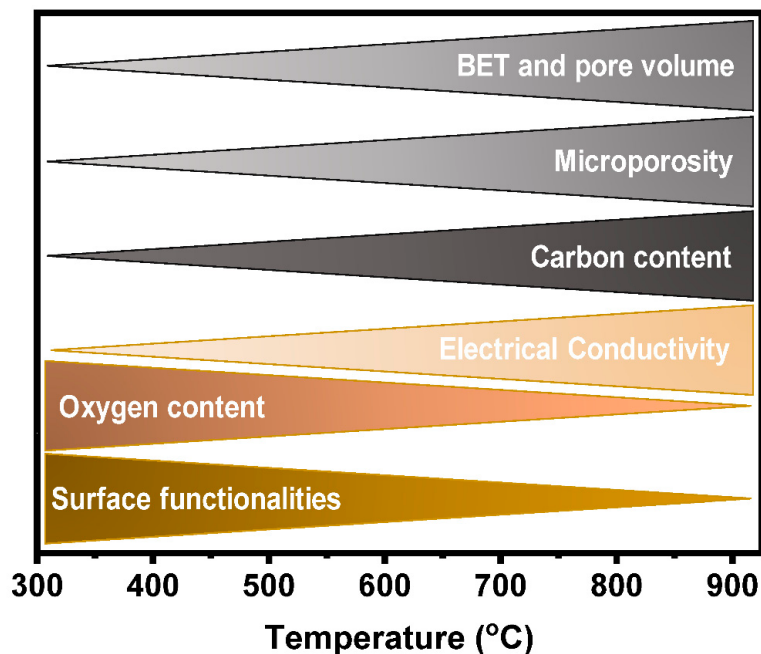


Figure 1. Pyrolytic temperature of biochar. Reproduced with permission from MDPI 2023 [5].

2.1. Pyrolysis

This process can be defined as the conversion of material at temperatures that are high without oxygen. Temperature, heating rate, and reaction time are known to have a direct influence on the biochar. Biomass goes through several temperature stages to allow appropriate decomposition into a carbon-rich material. Carbon monoxide and carbon dioxide volatilisation occur at 100 degrees Celsius and at around 200 degrees Celsius, respectively, and hemicellulose, hexoses, and pentoses begin to decompose [18–21].

Cellulose will then decompose at around 240 degrees Celsius. The final component, lignin, breaks down at temperatures below 500 degrees Celsius. This eliminates all volatile components, such as CH_4 . This will result in a solid black powder, which is biochar. It has low crystallinity, surface area, and pore volume. Another study shows that slow pyrolysis yields carbon (78.34–56.3%) between 200 and 500 °C. It is vital that temperatures do not exceed 500 degrees Celsius; otherwise, they begin to form silica, which is an undesirable product [22–26].

2.2. Activation

Biochar can be activated both chemically and thermally. Heat treatment thermally activates biochar in a furnace, as mentioned above, and acidic/basic matrix chemically activates the biochar. The main purpose of activation is to improve the chemical and physical properties of the product. This method can also, in other words, be said to be cracking, which simply involves breaking up the biomass into carbon and hydrogen [17,27,28].

Therefore, the activation of the biochar chemically also needs to be washed after the acids react with it to achieve a neutral pH, which is vital for the functioning of the battery and to remove any impurities that may have formed during the activation process. Chemical activation has far more advantages than thermal activation because of its short activation time, low temperature, high surface area, and high reactivity. Potassium hydroxide is the best activator, as it delivers the highest yield [28,29].

Equations (1)–(3) were used to calculate the product yield. Previously, similar expressions were used, where m_1 denotes the mass of the feed chamber + feed (in grammes), m_2 is the mass of the feed chamber, and m_3 is the weight of the feed chamber + product. Data

($m_1 = 600$ g, $m_2 = 480$ g, and $m_3 = 500$ g) were obtained from a single sugarcane bagasse conversion. The researchers reported biochar yields from the values obtained, which are summarised in Table 1.

$$m_{\text{Biochar}} = (m_3 - m_2) \quad (1)$$

$$m_{\text{Biochar}} = (m_1 - m_2) \quad (2)$$

$$\text{Yield}_{\text{Biochar}} = \frac{m_{\text{Biochar}}}{m_{\text{Raw}}} \times 100\% \quad (3)$$

Table 1. Comparative study on biochar production from various feedstocks.

Biomass Waste	Optimal Temperature (°C)	Duration (min)	Product Yield (wt%)	References
Sugarcane bagasse ash	349	70	16.67	[30]
Orange Peel	300	120	-	[31]
Orange albedo	300	120	-	[31]
Elephant grass	300	120	14.29	[32]
Palm oil fibres	387	80	15.9	[33]
Plantain fibres	220	150	6.98	[34]

The researchers recorded the results tabulated in Table 1, in which six different feedstocks were investigated under the same practical conditions. Based on the results, it is worth noting that biochar derived from sugarcane bagasse ash was more effective. Furthermore, nontabled textural properties revealed that the biochar yield of sugarcane bagasse ash was high quality, with a significantly greater surface area than its counterparts specific to BET [28,35–38].

The carbon feedstock, Norway spruce bark, was pretreated with $ZnCl_2$ and KOH for biochar 1 and biochar 2, respectively. Biochar materials were exposed to 800 °C for 2 h in a tube furnace under nitrogen atmosphere. The post-treatment involved the use of diluted 6 M HCl and 1 M HCl for biochar 1 and biochar 2, respectively. The biochars underwent vacuum filtration and then were washed several times and decanted until the supernatant reached an approximate value of 6.5. The textural properties of biochar 1 and 2 were investigated using N_2 adsorption–desorption at 77 K, as shown in Figure 2a,b. From the isotherm analysis, biochar 2 (Figure 2b) showed the existence of micropores in the material ascribed to N_2 adsorption, as no hysteresis loop was observed, although a hysteresis loop was observed for biochar 1, in the range of 0.4 and 0.6, indicating mesopores in the material. The results indicate that biochar 1 treated with $ZnCl_2$ exhibits mesopores, while biochar 2 treated with KOH exhibits micropores at low relative pressures [39–42].

Morphological studies were also performed, as shown in Figure 2c,d, in which both materials showed macropores, and most ultra-macropores can be observed in Figure 2c. The macropores facilitate the permeation of the electrolyte following charge accumulation into the cavities. Figure 2d shows the rough surface and irregular structure with small holes. It is evident that the activation of these materials was significant. Lastly, the structural properties of the biochars were studied, and the degree of graphitisation was also observed in the biochars. The structural defects and disorder of the carbon materials were more prominent in biochar too, which means that the hybridisation of sp^2 was low and highly disordered at the D peak was larger than the G peak, as shown in Figure 2f. The degree of graphitisation can be observed in Figure 2e, implying that activation with $ZnCl_2$ induces graphitic fragments and thus more sp^2 electronic domains of sp^2 in the structure, with the peak of G being larger than that of D [39,42–45].

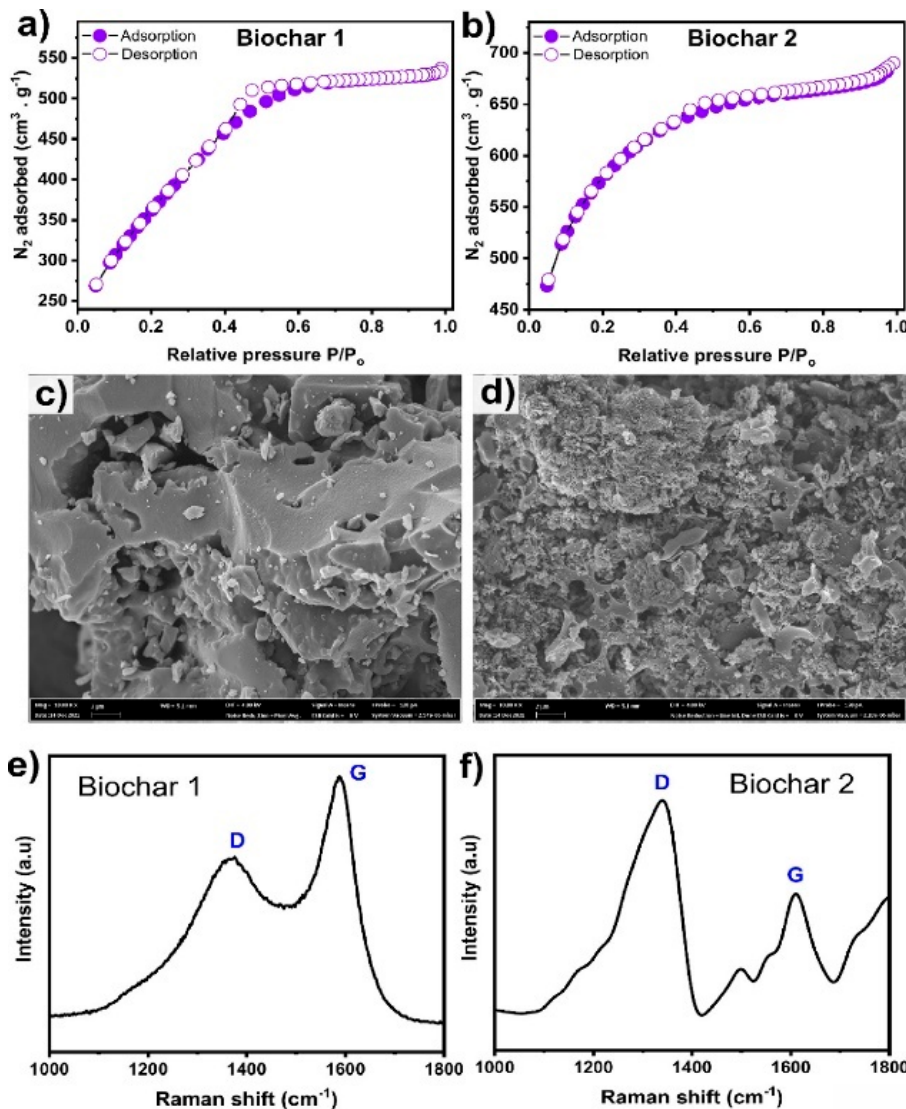


Figure 2. Properties of chemically impregnated biochar 1 and biochar 2: (a,b) adsorption–desorption isotherms of N₂, (c,d) FESEM images, and (e,f) Raman analysis. Reproduced with permission from [42], copyright 2022.

3. Biochar Characteristics

Biochar has several origins that can influence its electrochemical efficiency. These include biomass from forestry, where during photosynthesis about a percentage of the sunlight is stored as chemical energy. This method is far from that of fossil fuels that burn old biomass to produce new carbon dioxide [46,47]. The next is waste from municipal waste systems; when it comes to waste from municipal drainage, it can be considered organic waste. Biochar derived from municipal waste usually has a high surface area, which improves storage in LIBs. Waste of this kind has always been used in fertilisers and composts [48].

There is also food waste and perishable waste, which contain a lot of valuable resources, for example, potassium, calcium, magnesium, etc. Animal waste, for example, fish scales, bones, and animal skin, is high in collagen and can be synthesised into a carbonaceous material upon pyrolysis. Eggshells are rich in nitrogen. Eggshells can be used to make carbon-rich material, which can then be used to synthesise anode material for LIBs. The eggshells, which are also very rich in calcium, can also be used to synthesise anode material in LIBs, which minimises issues that may arise with electrode degrading due to electrolytes [49,50].

Silicon, potassium, and nitrogen are some of the elements found in perishable waste that therefore contribute to the conductivity of carbon biochar. The next is waste from agriculture. This refers to crop waste left over after harvest, for example, straw stems and bagasse, stalks, and leaves. Annually large amounts of agricultural waste are produced; the main contributors are maize, wheat, rice, sugar cane, cotton, and beans, as shown in Figure 3. These agricultural residues are not only a good source of carbon but also serve as self-doping for heteroatoms [51–53].



Figure 3. Several forms of biomass waste produced in agriculture. Reproduced with permission from [38], © 2020 Elsevier Ltd.

Agriculture waste is the most abundant waste and is produced in large amounts throughout the world. Therefore, it adds significantly to the amount of pollution that affects the environment. In South Africa, sugarcane bagasse contributes greatly to pollution in the country. Sugarcane is grown and harvested in KZN, and if it is not properly disposed of, it attracts insects that affect air quality and further affect future harvests. Sugar cane waste consists of potassium, phosphorus, methionine, and cysteine [50–53]. In this review, further studies look at sugar-cane-derived biochar, not only because of its physicochemical properties but also because it is the waste that is produced the most abundantly in South Africa [38,54,55].

3.1. Elemental Composition of Biochar

Biochar consists of carbon, oxygen, nitrogen, hydrogen, and sulphur. During pyrolysis, the composition of each of these heteroatoms is significantly reduced. Since the charring process is closely related to the functional groups present, it is important to explore them. The main functional group consists of mainly carbon-containing groups, for example, carboxylic acids, hydroxyls, phenolics, and carbonyls. These functional groups may be found in actual biomass or in the pyrolyzed product [46–49,56].

3.2. pH and Surface States

When the biochar was analysed for functional group contents and pyrolysis temperatures, it was found that with an increase in the use of pyrolysis temperatures, there would be an increase in pH. High temperatures will produce conductive biochar, whereas at low temperatures, acidic biochar is produced. Surface charge can be defined as the difference in conductivity between the internal and external parts of the biochar. The pH of a matrix can tailor the surface charge of a material. And the electron-donating capacity of Biochar was shown to increase with increasing temperature, but not at temperatures of about 500 degrees Celsius [46–55,57].

3.3. Surface Area

This property of biochar or most material being used as anode material is crucial in the overall performance of the device. Biochar is capable of hosting as many ions as possible. The size of the pores in the biochar dictates how large an ion can be trapped. Biochar with a small pore size cannot trap large substances. Larger pores and larger surface areas can be achieved at higher pyrolysis temperatures, and the porous structure of biochar can offer a larger surface area, thus storing a lot more lithium ions, regardless of where it is used [56,57]. Table 2 shows the different ways in which biomass can be used in lithium-ion batteries. Also, it offers some of the properties that make this biochar a specific part of the battery [58].

Table 2. The uses and functions of biochar made from biomass in LIBs.

Roles of Biomass-Derived Carbon in LIBs	Biochar Types	Properties of Biomass	Ref.
Anode material	Hard/soft carbon Activated carbon	SP ³ hybridised carbon sites, porosity, conductivity.	[38]
Dopant	Chitosan	Foreign atoms N and O	[38]
Binder	Chitin, Chitosan	Polymeric composition, chemically stable	[38]
Separator	Cellulose	Nonconductive, mechanically flexible, chemically stable	[38]
Current collector	Carbon cloth	Conductive thin film, mechanically flexible, and chemically organised	[38]

Carbonaceous materials derived from biomass have been widely and highly recognised, especially because they are raw materials for high-performance anode materials. In the quest to develop environmentally friendly and economically viable sustainable materials, Table 3 represents the various feedstock methodologies and their electrochemical performances. Biochars are low-cost and derived from various feedstocks; and they offer a wide range of excellent properties. Biochar-derived bagasse performed significantly higher than its counterparts, with an initial capacity of 2347.56 g⁻¹ [58].

Table 3. Electrochemical performance of carbon-based anodes for LIBs.

Feedstock	Synthetic Route	Initial Capacity (mA h g ⁻¹)	Ref.
Mustard seed	Hydrothermal	~822	[5]
Rice straws	High temperature	2041	[59]
Bagasse	Hydrothermal	2347.56	[29]
Banana peel	High temperature	~2150	[60]
Wood	Ball milling and pyrolysis	~315	[61]
Grass pollen	Pyrolysis	788.99	[62]
Coffee waste	Dry mechanochemical grinding	764	[63]
Sisal fibre	Hydrothermal	646	[64]

4. Energy Storage Systems

Energy can be generated, transmitted, converted, and stored when necessary. Now more than ever, it has become important to store energy, but this can be difficult. This may require bulky and expensive equipment. The main goal of many of today's energy storage systems is not only to have high performance but also to have a cheap and long-lasting life. These energy storage devices should also have no negative impact on the environment. The type of energy being stored determines a suitable energy device. Energy storage systems consist of a storage area and an energy conversion region [65,66]. The energy storage unit

can be operated with the use of an inverter. For others, a rectifier converts the alternating current to direct current [67–71].

4.1. Operational Principles of LIBs

Lithium-ion batteries also have high efficiency and performance, are lightweight, and have a high storage capacity [1]. Several cells must be placed in series to obtain direct voltage and capacity. Normal functioning needs to be considered, since there is a positive terminal called the cathode, where charge happens, and a negative terminal called the anode, where oxidation occurs when discharging. Both the anode and the cathode are soaked in the electrolyte with a separator included to separate them [4,70,71].

They can deliver the same or greater energy at half the size and weight. Unlike lead-acid batteries, they do not charge in stages. Temperature fluctuations or energy depletion do not affect the power output of lithium-ion batteries. Unfortunately, the reason that LIBs have such low overall application is due to the high price and safety issues they pose. One way to solve this problem is to develop their anode material. The most suitable is biochar, as it is derived from renewable biomass [72,73].

Inside the device, a redox reaction is taking place; reaction (4) denotes the lithiation of cobalt oxide (cathode) and reaction (5) the delithiation of graphite (anode). Lastly, reaction (6) describes the overall mechanism:



The lithiation process or charge is represented in reaction (4), and delithiation is shown in reaction (5), which depicts the discharge process. During charging, emitted Li^+ travels from the cathode and is delivered to the anode, whereas during discharge, the opposite takes place. Graphite has also been a satisfactory conductive anode material and is not costly to prepare, making it a viable anode material [4]. It has been reported that its capacity is very close to its theoretical maximum, and it is important to develop a much higher capacity. Unfortunately, poor performance rates hindered the significant development of LIBs. To improve lithium-ion batteries, new carbon-rich materials must be introduced [65–73].

4.2. Biochar in LIBs

Low-cost and ecologically friendly carbon obtained from biomass can be useful for lithium-ion batteries. This section shows the impact of pristine and doped carbon matrices from various sources and analyses their electrochemical performance.

Researchers report the slow catalytic pyrolysis of green toxic macroalgae to produce biochar. The magnetic biochar generated in the presence of iron as a catalyst exhibited exceptional textural qualities, with a specific surface area of $296.4 \text{ m}^2/\text{g}$. Cyclic voltammetry was performed on biochar in Figure 4a and magnetic biochar in Figure 4b during the 2nd, 10th, and 50th cycles, with a scan rate of 0.05 mV s^{-1} . Half-cells exhibited typical CV curves for carbon-based anode materials in LIBs. Furthermore, the electrode materials demonstrated strong reversible reactions and stability based on the observable overlaps between the two cycles. The area of the CV curves in both electrodes was determined, and magnetic biochar had a high area under the CV curves, which is attributable to Fe concentration; consequently, doping with Fe increases the capacity of anode materials in Li-ion batteries [74–76].

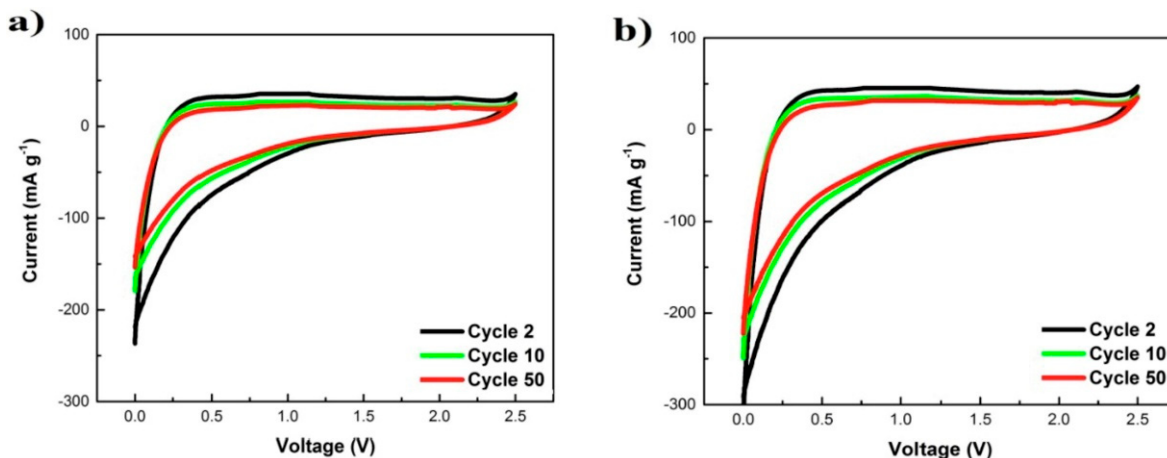


Figure 4. CV profiles of (a) biochar and (b) magnetic biochar. Reproduced with permission from [76], © 2019 Elsevier Ltd. All rights reserved.

In a novel and intriguing study, green poisonous macroalgae—a naturally occurring resource—was used as feedstock for lithium-ion batteries (Figure 5a–d). First, the waste material was used to create Fe (III)-decorated algae. After being doped with Fe (III), the pyrolytic feedstock was utilised to create magnetic biochar. As a result, research on LIBs produced some interesting findings, including an increase in surface area and electroactive sites, which increased capacity (see Table 4). They conducted a comparative analysis and found that the magnetic biochar capacity (91%) was double that of pure biochar (62%). This work could lead to a breakthrough in the development of environmentally benign and alternative magnetic materials for use in low-cost and clean energy systems [76].

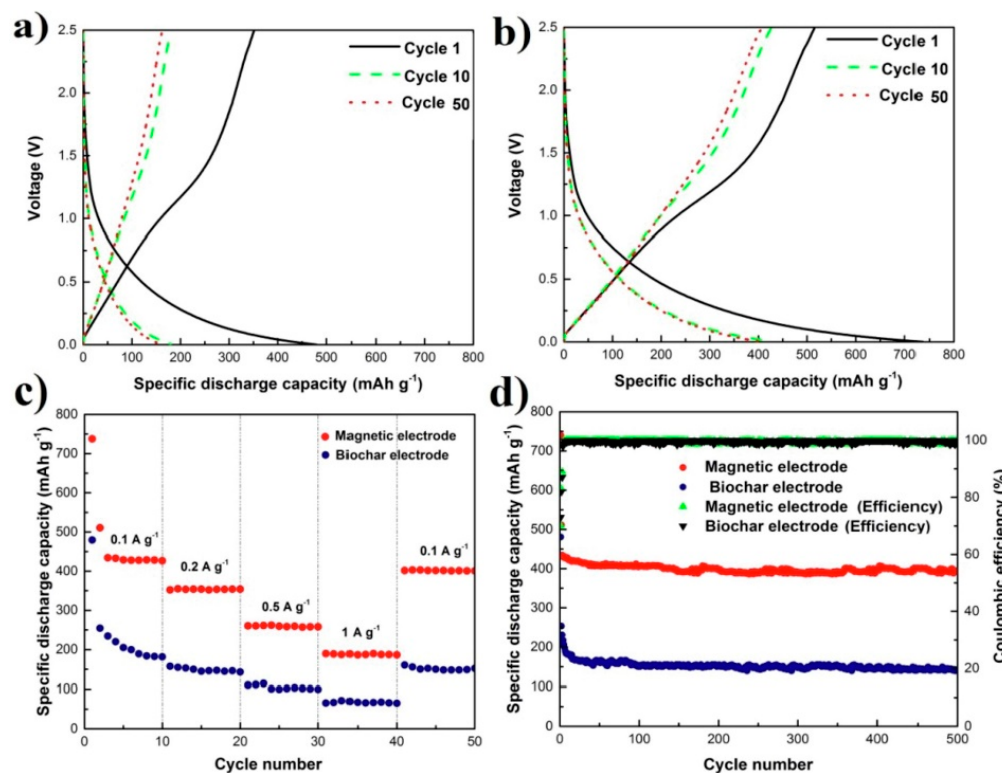


Figure 5. Charge–discharge investigation of (a) biochar and (b) magnetic biochar, (c) capacity as a function of current density, and (d) cycling curves. Reproduced with permission from [76], © 2019 Elsevier Ltd. All rights reserved.

Thus, carbon-rich biochar can contribute several advantages, namely increased porosity, which leads to increased Li-ion storage capacity. The morphological benefit of biochar is that it offers a high specific surface area, allowing for the increased storage of lithium ions. Biochar also increases the diffusion rate. This increases the discharge and charge rates. Biochar increases the stability and longevity of lithium-ion batteries, enhances the stability of the anode material over repeated cycles, and mitigates issues that may arise, such as fading capacity. The use of biochar is also environmentally friendly, as it uses renewable biomass as a direct feedstock [77].

Researchers have revealed interesting findings (see Table 4, Figure 6A–D, on porous carbon generated from nitrogen-doped human hair. According to reports, the study was the first to synthesise anode material from the human hair hydrothermal carbonization process, and it outperformed other biomass-based carbon compounds in terms of electrochemical properties. This was thought to be related to the carbon porosity (3–24 nm range) and graphitic nanosheet fragments, the large specific surface area of $1617 \text{ m}^2 \text{ g}^{-1}$, and the presence of a foreign atom, nitrogen. This was a low-cost, environmentally friendly innovative material for LIBs [78–80].

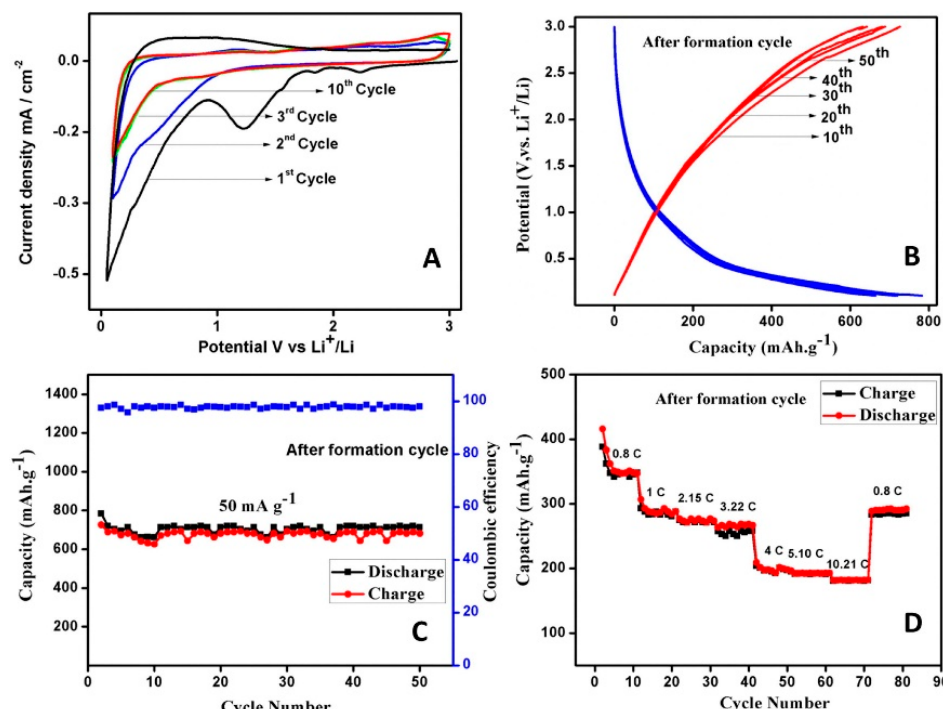


Figure 6. (A) CV curves of carbon derived from human hair, (B) charge–discharge profiles, (C) capacity retention, and (D) capacity as a function of current density. Reproduced with permission from [80], Copyright © 2014 Elsevier Ltd.

In a typical pyrolysis method, carbon was produced from soybean milk as the precursor material which underwent high temperatures ($600\text{--}800\text{ }^\circ\text{C}$) in an inert atmosphere of nitrogen. Figure 7a–d depicts the electrochemical analysis of carbon produced from soybean milk as a source. This material demonstrated a high degree of graphitisation with interconnected nanosheets suited for Li insertion, owing principally to the heteroatom nitrogen, which improved the rate performance in LIBs for ultrathin carbon nanosheets. The excellent Li-ion insertion capacity of this material and the reversible capacity (see Table 4) make it a promising candidate for portable energy storage devices. The presence of heteroatoms in the carbon matrix determines the degree of graphitisation [81–83].

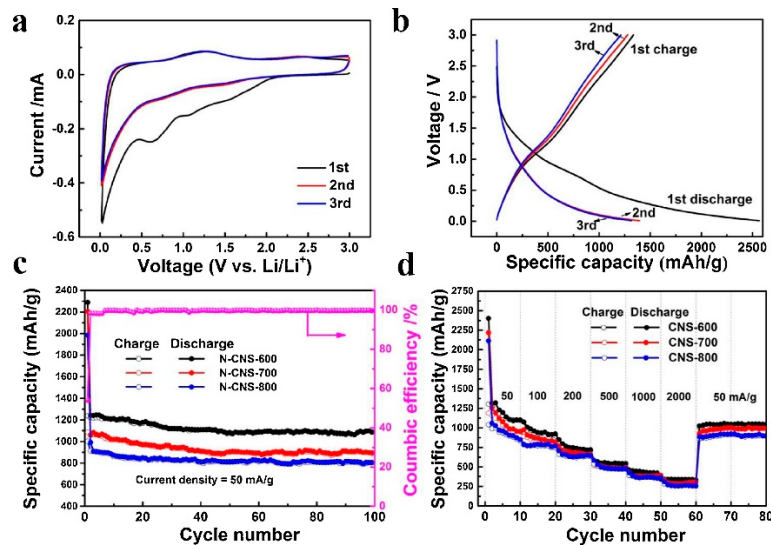


Figure 7. (a) CV analysis, (b) charge–discharge profiles, (c) cycling, and (d) capacity as a function of current density. Reproduced with permission from [83], © 2017 Elsevier B.V.

The carbon derived from sisal fibres via hydrothermal activation was tested for electrochemical indicators in LIB half-cells. And the intercalation capability was shown to be fairer in treated carbon than in untreated carbon, as shown in Figure 8. The greater insertion capacity (see Table 4) in treated carbons results from the presence of additional nanopores in the treated material. However, the minor inadequate capacity during cycling is due to structural flaws originating from nanodomains, such as dangling bonds, which are primarily the sp^3 hybridised carbon of sp^3 . Biomass annealing or pyrolysis causes disturbances in sp^2 bonding [63,84].

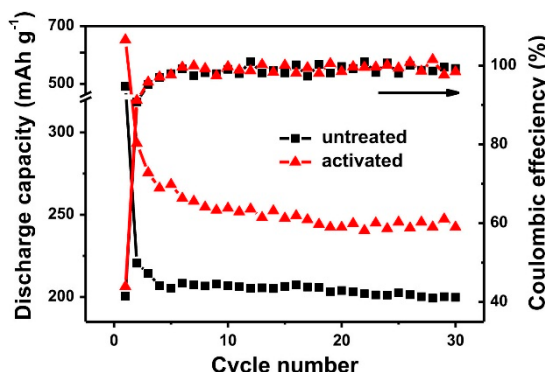


Figure 8. Cyclic and Coulombic profiles of the prepared electrodes. Reproduced with permission from [63], Copyright © 2014 Elsevier B.V.

The carbon material created from the biomass was examined, and the cycling results were obtained (Figure 9a,b). Figures 7b and 9a depict the first cycles of untreated and treated carbon, respectively. The reported data demonstrated that the discharge–charge curves of the manufactured electrode materials had much higher theoretical capacity values than those of graphite, owing to the degree of disorder in the carbon material. As previously stated, the amorphous carbon was added through pyrolysis rather than improved graphitisation. Furthermore, capacity losses have been reported, which can be accounted for by SEI film degradation on the electrode surface and irreversible Li insertion because of chemically adsorbed hydroxyl molecules on the surface of the microporous carbons. Biomass has a strong Li insertion capacity and cycle stability; see Table 4. Interestingly, Figure 5 shows that carbon-based biomass has a high Li insertion capacity and cycling stability [63,84].

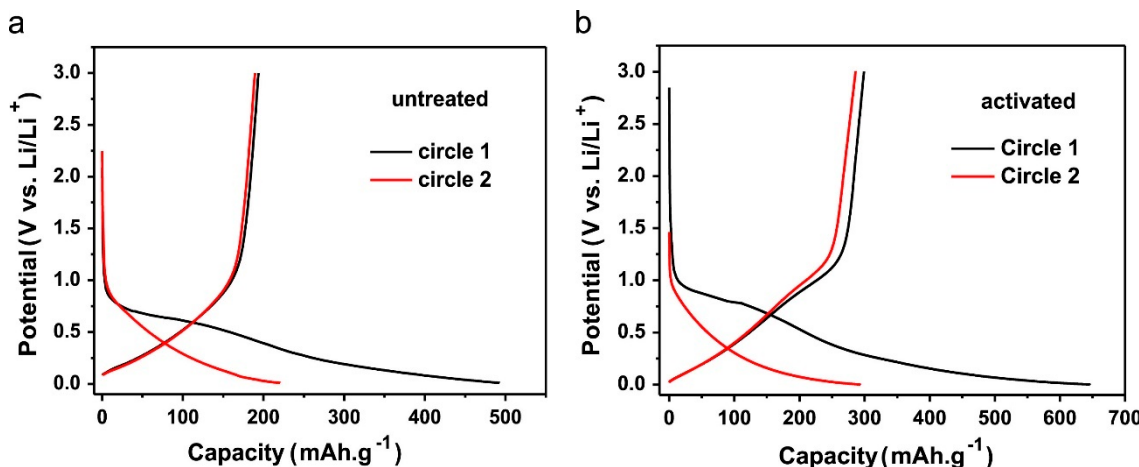


Figure 9. Charge–discharge profiles of (a) pristine and (b) pretreated carbon. Reproduced with permission from [63], Copyright © 2014 Elsevier B.V.

Biomass research is a robust sector that produces useful and valuable products. The study used a feedstock from bamboo chopsticks as a carbon source and was exposed to a hydrothermal synthetic route in alkaline media to produce biochar. Figure 10A–D shows the findings of a study on bamboo-derived carbon fibres. Figure 10A shows the CV analysis of cathodic behaviour throughout an increasing voltage window, which is mostly linked with Li intercalation into the carbon matrix. The disappearance peak in reduction is caused by irreversible reactions, including SEI degradation in carbon fibres. The feedstock was utilised to make carbon fibres, which were then carbonised to incorporate graphitic pieces. The material was further examined for electrochemical performance in LIBs and demonstrated improved rate capabilities (see Table 4). The researchers next grew MnO_2 atop the carbon matrix to build a 3D core shell with synergistic effects, which led to the excellent cycling performance of the hybrid electrode material. The good anode material for LIBs is the result of the synergistic effects of nanostructured metal-based oxide(s) anchored to the carbon matrix [84–88].

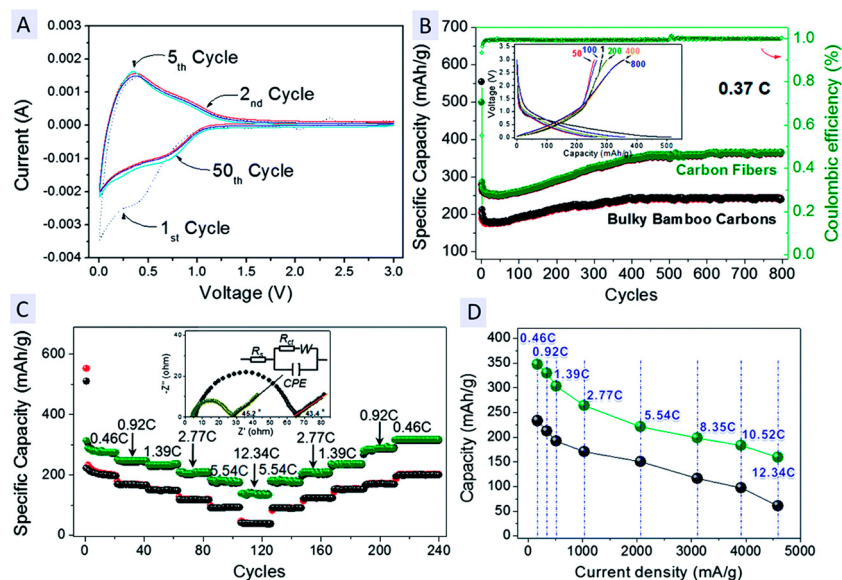


Figure 10. Carbon from bamboo, (A) CV curves, (B) cycling, (C) charge–discharge curves, and (D) capacity as a function of current density. Reproduced with permission from [88], © The Royal Society of Chemistry 2014.

Table 4 evaluates the identification of biomass and the electrochemical examination of the carbon extracted from it. Table 4 highlights the electrochemical output of biochar materials derived from spruce trees, sisal fibre, sugarcane bagasse, macroalgae, bamboo, soybeans, gelatine, and human hair. The results indicate that biochar is electroactive and can be fine-tuned to extract the most electrochemistry properties from the substance. The biochar produced from bagasse showed an excellent capacity of 1662 mAh g^{-1} , indicating that this feedstock can be used for industrial purposes in the energy storage sector [89].

Table 4. Electrochemical performance of carbon-based biomass as anode material.

Biomass.	Rate Capability (mA g^{-1})	Cycles	Capacity (mAh g^{-1})	Capacity Retention	Ref.
Spruce tree	100, 500, 1000	100, 1000, 5000	370, 332.4, 319	98.50	[42]
Sisal fiber	-	-	492/646 (T)	-	[63]
Sugarcane bagasse	100	600	1662	80.2	[89]
MacroAlgae	-	500	740	-	[76]
Bamboo chopsticks	-	300	710	-	[87]
Soybean Milk	50	100	1084	-	[83]
Gelatin	-	200	600	-	[90]
Human hair	50, 100	50	700, 610	-	[80]

4.3. Prospects

Greener and more cost-effective methods for processing sustainable batteries must be developed. Interesting results are reported in Table 5. The morphology and structural properties of carbonaceous materials affect electrochemical performance, whereby the structurally dejected carbon displayed the lowest rate, and the cherry pit exhibited excellent capacities, largely due to the porosity associated with these hard carbons [38,61,63,91,92].

Table 5. The electrochemical output of carbonaceous-based biomass materials.

Source of Biomass	Morphology	Specific Surface Area ($\text{m}^2 \text{ g}^{-1}$)	Initial Discharge–Charge Capacity Yield (mAh g^{-1})	Cycles/Rate Capability (mAh g^{-1})	Ref.
Wood	Hard	61	400/250	100/4 C	[92]
Sisal fiber	Honeycomb	103.5	1037/414	-	[93]
Jute fiber	Micro-meso	1028.6	1173/534.1	310.4/1.86	[94]
Plant tree leaves	Porous	518.6	906.2/460.4	242.7/2 A	[63]
Tamarind plant seeds	porous	103.5	1037/414	-	[95]
Cherry pit	Dejected	1662	1300/300	70/1.86 A	[96]

To produce porous carbon material, plane tree leaves were pyrolysed at temperatures between 500 and 800 °C in an inert atmosphere. The discharge–charge curves of carbon-based biomass that was calcined at 500, 600, 700, and 800 °C are shown in Figure 11. The primary cause of the first loss of capacity is the abundant carbon pores due to electrolyte breakdown and surface hydrogenation, which traps lithium ions and fills the gaps [95]. The best specific surface area and maximum Coulombic efficiency were found in carbon calcined at 700 °C, indicating that porous materials aid in the intercalation and deintercalation of the reversible lithium cycle. Furthermore, calcined carbon at 800 °C has charge voltages of about 1.0 V, which is different from 600 and 700 °C. This difference in charging voltages encourages lithiation through pore channels and a high specific surface area [96,97].

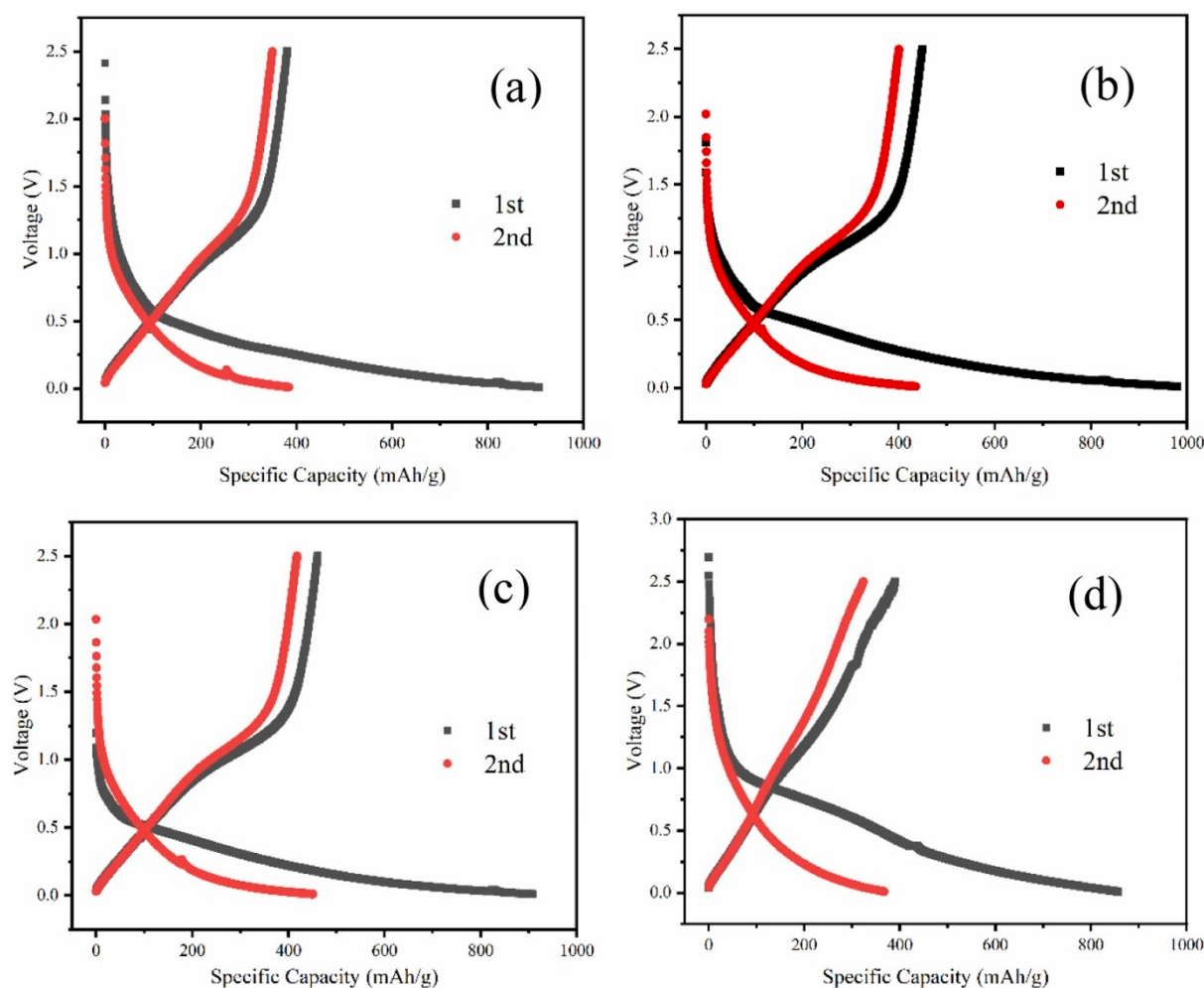


Figure 11. Electrochemical output of carbon pyrolysed at different temperatures: (a) 500 °C, (b) 600 °C, (c) 700 °C, and (d) 800 °C at 0.05 A g⁻¹ potential sweep 0.01 V–2.5 V. Reproduced with permission from [97] © 2024, Elsevier.

The use of biogenic carbon (biochar) has the potential to accelerate research on alternatives to greener materials, but it also has the potential to effectively address important challenges, such as improving the electrochemical output of these technologies [97,98]. Pretreatment of carbon from biomass, depending on the type of feedstock, can increase electron and ion transportation. The increased surface area and porosity of carbon-based biomass are often ascribed to the excellent electrochemical properties of these carbonaceous materials, hence their potential application in fuel cell technology, supercapacitors, and adsorbents. Therefore, an entirely bioderived energy storage device is critical. Despite all the benefits, the following challenges remain [97–101]:

Inadequate understanding of the behaviour of biomass-based carbon at the molecular and electronic level. Materials generated from biomass, such as multidimensional inorganic carbons, can help create more sustainable battery systems and components [101]. This study has provided evidence that biochar has a future in energy storage devices and conversion.

- I. The chemistry of various biomass sources should be further and extensively studied to better understand the low cost and quality of biomass to yield significant and promising battery performance.
- II. Surface science study is also required to better take impurities or residuals to a negligible level in biomass-derived carbon. Sophisticated techniques to explain the chemistry of these carbonaceous nanomaterials from atomic and molecular structure will aid in theoretical and experimental studies.

- III. A window of opportunity in this area is to opt for a tailored atomic structure of carbon derived from biomass. In the future, upcoming authors may look at other forms of biomass that could potentially offer improved performance.

5. Conclusions

Biomass carbon-based material is critical as new plans are established to reduce the predominant use of fossil fuels. Biochar, which can be obtained from a variety of sources, has been proven to be an effective substance, because it is readily available, abundant, and inexpensive. To replace or compete with the current graphite anode, biochar demonstrated increased energy storage capacity, stability, and overall cyclability, which are discussed in this paper. However, research to realise possible practical applications in commercial LIBs is still in its infancy stage.

Biochar obtained from agricultural waste, the most prevalent waste generated, has been found to improve the efficiency and capacity of LIBs. This study demonstrated that biochar might be used as a lithium-ion anode material. Furthermore, doping or surface functionalisation of biochar with foreign or heteroatoms enhances its electrochemical performance as an anode material. Carbon from renewable feedstocks or biomass ensures low-cost and environmentally friendly procedures. As a result, it has pioneered the creation of clean, low-cost energy storage devices. The physicochemical properties of biochar combined with its electrochemical performance show that Li-ion storage capacity can be improved by its textural properties, which emphasises that biochar has intercalating strengths, as this review was able to prove.

Funding: The financial assistance of the National Research Foundation (NRF), grant number (138079) and Eskom, grant number (2002/015527/0), South Africa, towards this research is acknowledged.

Acknowledgments: This research was supported by the Electrochemical Energy Technology Research Group, the Energy Centre, at the CSIR, and the Sustainable and Renewable Energy Nanomaterials Research Group, the University of the Western Cape.

Conflicts of Interest: The authors declare no conflicts of interest.

References

1. Nayak, P.K.; Yang, L.; Brehm, W.; Adelhelm, P. From lithium-ion to sodium-ion batteries: Advantages, challenges, and surprises. *Angew. Chem. Int. Ed.* **2018**, *57*, 102–120. [[CrossRef](#)] [[PubMed](#)]
2. Bae, H.; Kim, Y. Technologies of lithium recycling from waste lithium-ion batteries: A review. *Mater. Adv.* **2021**, *2*, 3234–3250. [[CrossRef](#)]
3. Xu, D.; Liang, M.; Qi, S.; Sun, W.; Lv, L.P.; Du, F.H.; Wang, B.; Chen, S.; Wang, Y.; Yu, Y. Progress and prospects of tunable organic molecules for organic lithium-ion batteries. *ACS Nano* **2020**, *15*, 47–80. [[CrossRef](#)] [[PubMed](#)]
4. Kane, S.; Storer, A.; Xu, W.; Ryan, C.; Stadie, N.P. Biochar as a renewable substitute for carbon black in lithium ion battery electrodes. *ACS Sustain. Chem. Eng.* **2022**, *10*, 12226–12233. [[CrossRef](#)]
5. Molaiyan, P.; Dos Reis, G.S.; Karuppiah, D.; Subramaniyam, C.M.; Garcia-Alvarado, F.; Lassi, U. Recent progress in biomass-derived carbon materials for lithium ion and Na ion batteries: A review. *Batteries* **2023**, *9*, 116. [[CrossRef](#)]
6. Muddasar, M.; Mushtaq, M.; Beaucamp, A.; Kennedy, T.; Culebras, M.; Collins, M.N. Synthesis of sustainable lignin precursors for hierarchical porous carbons and their efficient performance in energy storage applications. *ACS Sustain. Chem. Eng.* **2024**, *12*, 2352–2363. [[CrossRef](#)] [[PubMed](#)]
7. Abe, H.; Murai, T.; Zaghib, K. Vapor-grown carbon fiber anode for cylindrical lithium ion rechargeable batteries. *J. Power Sources* **1999**, *77*, 110–115. [[CrossRef](#)]
8. Li, W.; Huang, J.; Feng, L.; Cao, L.; Ren, Y.; Li, R.; Xu, Z.; Li, J.; Yao, C. Controlled synthesis of macroscopic three-dimensional hollow reticulate hard carbon as long-life anode materials for Na-ion batteries. *J. Alloys Compd.* **2017**, *716*, 210–219. [[CrossRef](#)]
9. Zhao, Y.; Feng, J.; Liu, X.; Wang, F.; Wang, L.; Shi, C.; Huang, L.; Feng, X.; Chen, X.; Xu, L.; et al. Self-adaptive strain-relaxation optimization for high-energy lithium storage material through crumpling of graphene. *Nat. Commun.* **2014**, *5*, 4565. [[CrossRef](#)]
10. Kong, X.; Zhu, Y.; Lei, H.; Wang, C.; Zhao, Y.; Huo, E.; Lin, X.; Zhang, Q.; Qian, M.; Mateo, W.; et al. Synthesis of graphene-like carbon from biomass pyrolysis and its applications. *Chem. Eng. J.* **2020**, *399*, 125808. [[CrossRef](#)]
11. Jin, C.; Nai, J.; Sheng, O.; Yuan, H.; Zhang, W.; Tao, X.; Lou, X.W.D. Biomass-based materials for green lithium secondary batteries. *Energy Environ. Sci.* **2021**, *14*, 1326–1379. [[CrossRef](#)]
12. Zhou, L.; Zhang, K.; Hu, Z.; Tao, Z.; Mai, L.; Kang, Y.M.; Chou, S.L.; Chen, J. Recent developments on and prospects for electrode materials with hierarchical structures for lithium-ion batteries. *Adv. Energy Mater.* **2018**, *8*, 1701415. [[CrossRef](#)]

13. Mahmood, N.; Tang, T.; Hou, Y. Nanostructured anode materials for lithium ion batteries: Progress, challenge and perspective. *Adv. Energy Mater.* **2016**, *6*, 1600374. [[CrossRef](#)]
14. Das, R.; Panda, S.N. Preparation and Applications of Biochar-Based Nanocomposite: A review. *J. Anal. Appl. Pyrolysis* **2022**, *167*, 105691. [[CrossRef](#)]
15. You, S.; Ok, Y.S.; Chen, S.S.; Tsang, D.C.; Kwon, E.E.; Lee, J.; Wang, H.C. A Critical Review on Sustainable Biochar System through Gasification: Energy and environmental applications. *Bioresour. Technol.* **2017**, *246*, 242–253. [[CrossRef](#)] [[PubMed](#)]
16. Lin, Y.; Li, F.; Zhang, Q.; Liu, G.; Xue, C. Controllable preparation of green biochar-based high-performance supercapacitors. *Ionics* **2022**, *28*, 2525–2561. [[CrossRef](#)]
17. Salimi, P.; Tieuli, S.; Taghavi, S.; Venezia, E.; Fugattini, S.; Lauciello, S.; Prato, M.; Marras, S.; Li, T.; Signoretto, M.; et al. Sustainable lithium-ion batteries based on metal-free tannery waste biochar. *Green Chem.* **2022**, *24*, 4119–4129. [[CrossRef](#)]
18. Bartoli, M.; Arrigo, R.; Malucelli, G.; Tagliaferro, A.; Duraccio, D. Recent advances in biochar polymer composites. *Polymers* **2022**, *14*, 2506. [[CrossRef](#)]
19. Malyan, S.K.; Kumar, S.S.; Fagodiya, R.K.; Ghosh, P.; Kumar, A.; Singh, R.; Singh, L. Biochar for environmental sustainability in the energy-water-agroecosystem nexus. *Renew. Sustain. Energy Rev.* **2021**, *149*, 111379. [[CrossRef](#)]
20. Sun, C.; Du, A.; Deng, G.; Zhao, X.; Pan, J.; Fu, X.; Liu, J.; Cui, L.; Wang, Q. Naturally nitrogen-doped self-encapsulated biochar materials based on mouldy wheat flour were used for silicon anode in lithium-ion batteries. *Electrochim. Acta* **2023**, *450*, 142269. [[CrossRef](#)]
21. Anand, A.; Kumar, V.; Kaushal, P. Biochar and its twin benefits: Management of crop residues and mitigation of climate change in India. *Renew. Sustain. Energy Rev.* **2022**, *156*, 111959. [[CrossRef](#)]
22. Kang, Z.; Jia, X.; Zhang, Y.; Kang, X.; Ge, M.; Liu, D.; Wang, C.; He, Z. A review on application of biochar in the removal of pharmaceutical pollutants through adsorption and persulfate-based AOPs. *Sustainability* **2022**, *14*, 10128. [[CrossRef](#)]
23. Li, M.; Lu, J.; Chen, Z.; Amine, K. 30 years of lithium-ion batteries. *Adv. Mater.* **2018**, *30*, 1800561. [[CrossRef](#)] [[PubMed](#)]
24. Zhao, J.; Zhu, M.; Pang, Y.; Wu, H.; Ding, S. Layered NiPS₃ nanoparticles anchored on two-dimensional nitrogen-doped biochar nanosheets for ultra-high-rate sodium-ion storage. *Compos. Commun.* **2022**, *29*, 100988. [[CrossRef](#)]
25. Adeniyi, A.G.; Abdulkareem, S.A.; Ighalo, J.O.; Onifade, D.V.; Sanusi, S.K. Thermochemical co-conversion of sugarcane bagasse-LDPE hybrid waste into biochar. *Arab. J. Sci. Eng.* **2021**, *46*, 6391–6397. [[CrossRef](#)]
26. Ma, C.; Wang, H.; Zhao, X.; Wang, X.; Miao, Y.; Cheng, L.; Wang, C.; Wang, L.; Yue, H.; Zhang, D. Porous Bamboo-Derived Carbon as Selenium Host for Advanced Lithium/Sodium–Selenium Batteries. *Energy Technol.* **2020**, *8*, 1901445. [[CrossRef](#)]
27. Zhou, X.; Chen, F.; Bai, T.; Long, B.; Liao, Q.; Ren, Y.; Yang, J. Interconnected highly graphitic carbon nanosheets derived from wheat stalk as high-performance anode materials for lithium ion batteries. *Green Chem.* **2016**, *18*, 2078–2088. [[CrossRef](#)]
28. Adeniyi, A.G.; Ighalo, J.O.; Onifade, D.V. Biochar production from elephant grass (*Pennisetum purpureum*) using an updraft biomass gasifier with retort heating. *Biofuels* **2019**, *12*, 1283–1290. [[CrossRef](#)]
29. Zheng, S.; Luo, Y.; Zhang, K.; Liu, H.; Hu, G.; Qin, A. Nitrogen and phosphorus co-doped mesoporous carbon nanosheets derived from bagasse for lithium-ion batteries. *Mater. Lett.* **2021**, *290*, 129459. [[CrossRef](#)]
30. Adeniyi, A.G.; Ighalo, J.O.; Onifade, D.V. Production of biochar from plantain fibres (*Musa paradisiaca*) fibers using an updraft biomass gasifier with retort heating. *Combust. Sci. Technol.* **2021**, *193*, 60–74. [[CrossRef](#)]
31. Adelodun, A.A.; Adeniyi, A.G.; Ighalo, J.O.; Onifade, D.V.; Arowoyele, L.T. Thermochemical conversion of oil palm fiber/LDPE hybrid waste to biochar. *Biofuels Bioprod. Biorefining* **2020**, *14*, 1313–1323. [[CrossRef](#)]
32. Sun, J.; Shu, X.; Guan, J.; Tong, G.; Ding, H.; Chen, L.; Zhou, N.; Shuai, Y. N, P, and O-coated biochar from phytoremediation residues: A promising cathode material for Li–S batteries. *Nanotechnology* **2022**, *33*, 215403.
33. Li, M.; Zhang, H.; Xiao, T.; Wang, S.; Zhang, B.; Chen, D.; Su, M.; Tang, J. Low-cost biochar derived from corncob as an oxygen reduction catalyst in air cathode microbial fuel cells. *Electrochim. Acta* **2018**, *283*, 780–788. [[CrossRef](#)]
34. Ren, B.; Zhang, X.; Wang, B.; Li, Y.; Zeng, X.; Zhang, X.; Fan, M.; Yang, X. Designed the formation of hierarchical core-shell NiCo₂S₄@NiMoO₄ arrays on cornstalk biochar as battery-type electrodes for hybrid supercapacitors. *J. Alloys Compd.* **2023**, *937*, 168403. [[CrossRef](#)]
35. Gu, X.X.; Kuang, L.Y.; Lin, J.; Qiao, S.; Ma, S.; Li, Y.; Wang, Q.; Dai, J.H.; Zhou, X.; Zhou, H.Y.; et al. Highly porous nitrogen-doped biochar nanosheets for high-performance Li–Se batteries. *Rare Met.* **2023**, *42*, 822–829. [[CrossRef](#)]
36. Wang, X.; Zhang, Y.; Chang, Q.; Wu, Y.; Lei, W.; Zou, Y.; Ma, Z.; Pan, Y. Porous biochar nanosheets loaded with Fe₃C particles accelerate electrochemical reactions and their applications in Li–S batteries. *Sustain. Energy Fuels* **2021**, *5*, 4346–4354. [[CrossRef](#)]
37. Magnacca, G.; Guerretta, F.; Vizintin, A.; Benzi, P.; Valsania, M.C.; Nistic, R. Preparation, characterisation, and environmental/electrochemical energy storage testing of low-cost biochar from natural chitin obtained by pyrolysis under mild conditions. *Appl. Surf. Sci.* **2018**, *427*, 883–893. [[CrossRef](#)]
38. Senthil, C.; Lee, C.W. Biomass-derived biochar materials as sustainable energy sources for electrochemical energy storage devices. *Renew. Sustain. Energy Rev.* **2021**, *137*, 110464. [[CrossRef](#)]
39. Reis, G.S.D.; Oliveira, H.P.D.; Larsson, S.H.; Thyrel, M.; Claudio Lima, E. A short review on the electrochemical performance of hierarchical and nitrogen-doped activated biocarbon-based electrodes for supercapacitors. *Nanomaterials* **2021**, *11*, 424. [[CrossRef](#)]
40. Morali, U.; Demiral, H.; Şensöz, S. Optimization of activated carbon production from sunflower seed extracted meal: Taguchi design of experiment approach and analysis of variance. *J. Clean. Prod.* **2018**, *189*, 602–611. [[CrossRef](#)]

41. Thue, P.S.; Umpierres, C.S.; Lima, E.C.; Lima, D.R.; Machado, F.M.; Dos Reis, G.S.; da Silva, R.S.; Pavan, F.A.; Tran, H.N. Single-step pyrolysis for producing magnetic activated carbon from tucumā (*Astrocaryum aculeatum*) seed and nickel (II) chloride and zinc (II) chloride. Application for removal of nicotinamide and propanolol. *J. Hazard. Mater.* **2020**, *398*, 122903. [[CrossRef](#)]
42. Simoes dos Reis, G.; Mayandi Subramaniyam, C.; Cárdenas, A.D.; Larsson, S.H.; Thyrel, M.; Lassi, U.; Garcia-Alvarado, F. Facile synthesis of sustainable activated biochars with different pore structures as efficient additive-carbon-free anodes for lithium-and sodium-ion batteries. *ACS Omega* **2022**, *7*, 42570–42581. [[CrossRef](#)]
43. Yuan, C.; Chen, M.; Zhu, K.; Ni, J.; Wang, S.; Cao, B.; Zhong, S.; Zhou, J.; Wang, S. Facile synthesis of nitrogen-doped interconnected porous carbons derived from reed and chlorella for high-performance supercapacitors. *Fuel Process. Technol.* **2022**, *238*, 107466. [[CrossRef](#)]
44. Hou, S.; Cai, X.; Wu, H.; Yu, X.; Peng, M.; Yan, K.; Zou, D. Nitrogen-doped graphene for dye-sensitized solar cells and the role of nitrogen states in triiodide reduction. *Energy Environ. Sci.* **2013**, *6*, 3356–3362. [[CrossRef](#)]
45. Wei, M.; Marrakchi, F.; Yuan, C.; Cheng, X.; Jiang, D.; Zafar, F.F.; Fu, Y.; Wang, S. Adsorption modeling, thermodynamics, and DFT simulation of tetracycline onto mesoporous and high-surface-area NaOH-activated macroalgae carbon. *J. Hazard. Mater.* **2022**, *425*, 127887. [[CrossRef](#)]
46. Yao, Y.; Wu, F. Naturally derived nanostructured materials from biomass for rechargeable lithium/sodium batteries. *Nano Energy* **2015**, *17*, 91–103. [[CrossRef](#)]
47. Vivekanandhan, S. Biochar supercapacitors: Recent developments in materials and methods. *Green Sustain. Adv. Mater. Appl.* **2018**, *2*, 223–249.
48. Azam, M.A.; Safie, N.E.; Ahmad, A.S.; Yuza, N.A.; Zulkifli, N.S.A. Recent advances of silicon, carbon composites, and tin oxide as new anode materials for lithium-ion battery: A comprehensive review. *J. Energy Storage* **2021**, *33*, 102096. [[CrossRef](#)]
49. Li, X.; Zhang, J.; Liu, B.; Su, Z. A critical review on the application and recent developments of post-modified biochar in supercapacitors. *J. Clean. Prod.* **2021**, *310*, 127428. [[CrossRef](#)]
50. Wang, T.; Kretschmer, K.; Choi, S.; Pang, H.; Xue, H.; Wang, G. Methods for the fabrication of porous carbon materials and separator membranes for lithium–sulphur batteries: Development and future perspectives. *Small Methods* **2017**, *1*, 1700089. [[CrossRef](#)]
51. Leng, L.; Liu, R.; Xu, S.; Mohamed, B.A.; Yang, Z.; Hu, Y.; Chen, J.; Zhao, S.; Wu, Z.; Peng, H.; et al. An overview of sulphur-functional groups in biochar from biomass pyrolysis. *J. Environ. Chem. Eng.* **2022**, *10*, 107185. [[CrossRef](#)]
52. Xiang, W.; Zhang, X.; Chen, J.; Zou, W.; He, F.; Hu, X.; Tsang, D.C.; Ok, Y.S.; Gao, B. Biochar Technology in Wehrmacht Treatment: Critical review. *Chemosphere* **2020**, *252*, 126539. [[CrossRef](#)] [[PubMed](#)]
53. Goud, M.; Raval, F. A sustainable biochar-based shape stable composite phase change material for thermal management of a lithium ion battery system and hybrid neural network modelling for heat flow prediction. *J. Energy Storage* **2022**, *56*, 106163.
54. Venkatachalam, C.D.C.; Sekar, S.; Sengottian, M.; Ravichandran, S.R.; Bhuvaneshwaran, P. Critical review of the production, activation, and morphological characteristic study of functionalised biochar. *J. Energy Storage* **2023**, *67*, 107525. [[CrossRef](#)]
55. Abed Hussein, B.; Mahdi, A.B.; Emad Izzat, S.; Acwin Dwijendra, N.K.; Romero Parra, R.M.; Barboza Arenas, L.A.; Mustafa, Y.F.; Yasin, G.; Thaeer Hammid, A. Production, structural properties nano biochar and effects nano biochar in soil: A review. *Egypt. J. Chem.* **2022**, *65*, 607–618.
56. Adeniyi, A.G.; Ighalo, J.O.; Onifade, D.V. Biochar from the thermochemical conversion of orange peel (*Citrus sinensis*) peel and Albedo: Product quality and potential applications. *Chem. Afr.* **2020**, *3*, 439–448. [[CrossRef](#)]
57. Kalinke, C.; de Oliveira, P.R.; Bonacin, J.A.; Janegitz, B.C.; Mangrich, A.S.; Marcolino-Junior, L.H.; Bergamini, M.F. State-of-the-art technologies and perspectives in the use of biochar for electrochemical and electroanalytical applications. *Green Chem.* **2021**, *23*, 5272–5301. [[CrossRef](#)]
58. Pramanik, A.; Chattopadhyay, S.; De, G.; Mahanty, S. Efficient energy storage in mustard husk-derived porous spherical carbon nanostructures. *Mater. Adv.* **2021**, *2*, 7463–7472. [[CrossRef](#)]
59. Zhang, F.; Wang, K.X.; Li, G.D.; Chen, J.S. Hierarchical porous carbon derived from rice straw for lithium-ion batteries with high-rate performance. *Electrochem. Commun.* **2009**, *11*, 130–133. [[CrossRef](#)]
60. Lotfabad, E.M.; Ding, J.; Cui, K.; Kohandehghan, A.; Kalisvaart, W.P.; Hazelton, M.; Mitlin, D. High-density sodium and lithium-ion battery anodes from banana peels. *ACS Nano* **2014**, *8*, 7115–7129. [[CrossRef](#)]
61. Drews, M.; Büttner, J.; Bauer, M.; Ahmed, J.; Sahu, R.; Scheu, C.; Vierrath, S.; Fischer, A.; Biro, D. Hard carbon anodes for lithium ion batteries. *ChemElectroChem* **2021**, *8*, 4750–4761. [[CrossRef](#)]
62. Kietisirirojana, N.; Tunkasiri, T.; Pengpat, K.; Khamman, O.; Intatha, U.; Eitssayeam, S. Synthesis of mesoporous carbon powder from gold beard grass pollen for use as an anode for lithium ion batteries. *Microporous Mesoporous Mater.* **2022**, *331*, 111565. [[CrossRef](#)]
63. Yu, X.; Zhang, K.; Tian, N.; Qin, A.; Liao, L.; Du, R.; Wei, C. Biomass carbon derived from sisal fibre as anode material for lithium-ion batteries. *Mater. Lett.* **2015**, *142*, 193–196. [[CrossRef](#)]
64. Xiao, Y.; Raheem, A.; Ding, L.; Chen, W.H.; Chen, X.; Wang, F.; Lin, S.L. Pretreatment, modification and applications of sewage sludge-derived biochar for resource recovery-A review. *Chemosphere* **2022**, *287*, 131969. [[CrossRef](#)]
65. Iwuozor, K.A.; Emenike, E.C.; Ighalo, J.O.; Omoarukhe, F.I.; Omuku, E.E.; Adeniyi, A.G. Review of the thermochemical conversion of sugarcane bagasse into biochar. *Clean. Mater.* **2022**, *6*, 100162. [[CrossRef](#)]

66. Yuan, S.; Lai, Q.; Duan, X.; Wang, Q. Carbon-based materials as anode materials for lithium-ion batteries and lithium-ion capacitors: A review. *J. Energy Storage* **2023**, *61*, 106716. [[CrossRef](#)]
67. Du, A.; Li, H.; Chen, X.; Han, Y.; Zhu, Z.; Chu, C. Recent research progress of silicon-based anode materials for lithium-ion batteries. *ChemistrySelect* **2022**, *7*, e202201269. [[CrossRef](#)]
68. Haghghi Mood, S.; Pelaez-Samaniego, M.R.; Garcia-Perez, M. Perspectives of engineered biochar for environmental applications: A review. *Energy Fuels* **2022**, *36*, 7940–7986. [[CrossRef](#)]
69. Mian, M.M.; Alam, N.; Ahommed, M.S.; He, Z.; Ni, Y. Emerging applications of sludge biochar-based catalysts for environmental remediation and energy storage: A review. *J. Clean. Prod.* **2022**, *360*, 132131. [[CrossRef](#)]
70. Uday, V.; Harikrishnan, P.S.; Deoli, K.; Zitouni, F.; Mahlknecht, J.; Kumar, M. Current trends in the production, morphology, and real-world environmental applications of biochar for the promotion of sustainability. *Bioresour. Technol.* **2022**, *359*, 127467. [[CrossRef](#)]
71. Yaashikaa, P.R.; Kumar, P.S.; Varjani, S.; Saravanan, A. A critical review on the biochar production techniques, characterisation, stability, and applications for circular bioeconomy. *Biotechnol. Rep.* **2020**, *28*, e00570.
72. Ling, H.Y.; Chen, H.; Wu, Z.; Hencz, L.; Qian, S.; Liu, X.; Liu, T.; Zhang, S. Sustainable bioderived materials for addressing critical problems of next-generation high-capacity lithium ion batteries. *Mater. Chem. Front.* **2021**, *5*, 5932–5953. [[CrossRef](#)]
73. Amalina, F.; Abd Razak, A.S.; Krishnan, S.; Sulaiman, H.; Zularisam, A.W.; Nasrullah, M. Biochar production techniques utilising biomass waste-derived materials and environmental applications—A review. *J. Hazard. Mater. Adv.* **2022**, *7*, 100134. [[CrossRef](#)]
74. Ryu, D.J.; Oh, R.G.; Seo, Y.D.; Oh, S.Y.; Ryu, K.S. Recovery and electrochemical performance in lithium secondary batteries of biochar derived from rice straw. *Environ. Sci. Pollut. Res.* **2015**, *22*, 10405–10412. [[CrossRef](#)] [[PubMed](#)]
75. Yu, W.; Wang, H.; Liu, S.; Mao, N.; Liu, X.; Shi, J.; Liu, W.; Chen, S.; Wang, X. N, O-codoped hierarchical porous carbons derived from algae for high-capacity supercapacitors and battery anodes. *J. Mater. Chem. A* **2016**, *4*, 5973–5983. [[CrossRef](#)]
76. Salimi, P.; Norouzi, O.; Pourhoseini, S.E.M.; Bartocci, P.; Tavasoli, A.; Di Maria, F.; Pirbazari, S.M.; Bidini, G.; Fantozzi, F. Magnetic biochar obtained through catalytic pyrolysis of macroalgae: A promising anode material for Li-ion batteries. *Renew. Energy* **2019**, *140*, 704–714. [[CrossRef](#)]
77. An, S.J.; Li, J.; Daniel, C.; Mohanty, D.; Nagpure, S.; Wood, D.L., III. The state of understanding of the lithium-ion-battery graphite solid electrolyte interphase (SEI) and its relationship to formation cycling. *Carbon* **2016**, *105*, 52–76. [[CrossRef](#)]
78. Liu, T.; Luo, R.; Qiao, W.; Yoon, S.H.; Mochida, I. Microstructure of carbon derived from mangrove charcoal and its application in Li-ion batteries. *Electrochim. Acta* **2010**, *55*, 1696–1700. [[CrossRef](#)]
79. Isaev, I.; Salitra, G.; Soffer, A.; Cohen, Y.S.; Aurbach, D.; Fischer, J. A new approach for the preparation of anodes for Li-ion batteries based on activated hard carbon cloth with pore design. *J. Power Sources* **2003**, *119*, 28–33. [[CrossRef](#)]
80. Saravanan, K.R.; Kalaiselvi, N. Nitrogen containing bio-carbon as a potential anode for lithium batteries. *Carbon* **2015**, *81*, 43–53. [[CrossRef](#)]
81. Kaskhedikar, N.A.; Maier, J. Lithium storage in carbon nanostructures. *Adv. Mater.* **2009**, *21*, 2664–2680. [[CrossRef](#)]
82. Shi, L.; Chen, Y.; Song, H.; Li, A.; Chen, X.; Zhou, J.; Ma, Z. Preparation and lithium-storage performance of a novel hierarchical porous carbon from sucrose using Mg-Al layered double hydroxides as template. *Electrochim. Acta* **2017**, *231*, 153–161. [[CrossRef](#)]
83. Guo, S.; Chen, Y.; Shi, L.; Dong, Y.; Ma, J.; Chen, X.; Song, H. Nitrogen-doped biomass-based ultra-thin carbon nanosheets with interconnected framework for High-Performance Lithium-Ion Batteries. *Appl. Surf. Sci.* **2018**, *437*, 136–143. [[CrossRef](#)]
84. Wei, Y.; Tao, Y.; Kong, Z.; Liu, L.; Wang, J.; Qiao, W.; Ling, L.; Long, D. Unique electrochemical behavior of heterocyclic selenium-sulfur cathode materials in ether-based electrolytes for rechargeable lithium batteries. *Energy Storage Mater.* **2016**, *5*, 171–179. [[CrossRef](#)]
85. Norouzi, O.; Di Maria, F. Catalytic effect of functional and Fe composite biochars on biofuel and biochemical derived from the pyrolysis of green marine biomass. *Fermentation* **2018**, *4*, 96. [[CrossRef](#)]
86. Javanbakht, M.; Omidvar, H.; Hosen, M.S.; Hubin, A.; Van Mierlo, J.; Berecibar, M. Development, retainment, and assessment of the graphite-electrolyte interphase in Li-ion batteries regarding the functionality of SEI-forming additives. *Iscience* **2022**, *25*, 103862.
87. Pol, V.G.; Thackeray, M.M. Spherical carbon particles and carbon nanotubes prepared by autogenic reactions: Evaluation as anodes in lithium electrochemical cells. *Energy Environ. Sci.* **2011**, *4*, 1904–1912. [[CrossRef](#)]
88. Jiang, J.; Zhu, J.; Ai, W.; Fan, Z.; Shen, X.; Zou, C.; Liu, J.; Zhang, H.; Yu, T. Evolution of disposable bamboo chopsticks into uniform carbon fibers: A smart strategy to fabricate sustainable anodes for Li-ion batteries. *Energy Environ. Sci.* **2014**, *7*, 2670–2679. [[CrossRef](#)]
89. Wang, B.; Wang, Y.; Peng, Y.; Wang, X.; Wang, N.; Wang, J.; Zhao, J. Nitrogen-doped biomass-based hierarchical porous carbon with large mesoporous volume for application in energy storage. *Chem. Eng. J.* **2018**, *348*, 850–859. [[CrossRef](#)]
90. Qu, Y.; Zhang, Z.; Zhang, X.; Ren, G.; Lai, Y.; Liu, Y.; Li, J. Highly ordered nitrogen-rich mesoporous carbon derived from biomass waste for high-performance lithium-sulfur batteries. *Carbon* **2015**, *84*, 399–408. [[CrossRef](#)]
91. Roy, J.J.; Rarotra, S.; Krikstolaityte, V.; Zhuoran, K.W.; Cindy, Y.D.I.; Tan, X.Y.; Carboni, M.; Meyer, D.; Yan, Q.; Srinivasan, M. Green recycling methods to treat lithium-ion batteries E-waste: A circular approach to sustainability. *Adv. Mater.* **2022**, *34*, 2103346. [[CrossRef](#)] [[PubMed](#)]
92. Dou, Y.; Liu, X.; Wang, X.; Yu, K.; Liang, C. Jute fiber based micro-mesoporous carbon: A biomass derived anode material with high-performance for lithium-ion batteries. *Mater. Sci. Eng. B* **2021**, *265*, 115015. [[CrossRef](#)]

93. Panda, M.R.; Kathribail, A.R.; Modak, B.; Sau, S.; Dutta, D.P.; Mitra, S. Electrochemical properties of biomass-derived carbon and its composite along with $\text{Na}_2\text{Ti}_3\text{O}_7$ as potential high-performance anodes for Na-ion and Li-ion batteries. *Electrochim. Acta* **2021**, *392*, 139026. [[CrossRef](#)]
94. Hernández-Rentero, C.; Marangon, V.; Olivares-Marín, M.; Gómez-Serrano, V.; Caballero, Á.; Morales, J.; Hassoun, J. Alternative lithium-ion battery using biomass-derived carbons as environmentally sustainable anode. *J. Colloid Interface Sci.* **2020**, *573*, 396–408. [[CrossRef](#)] [[PubMed](#)]
95. Zhang, W.; Yin, J.; Lin, Z.; Lin, H.; Lu, H.; Wang, Y.; Huang, W. Facile preparation of 3D hierarchical porous carbon from lignin for the anode material in lithium ion battery with high rate performance. *Electrochim. Acta* **2015**, *176*, 1136–1142. [[CrossRef](#)]
96. Yu, K.; Zhang, Z.; Liang, J.; Liang, C. Natural biomass-derived porous carbons from buckwheat hulls used as anode for lithium-ion batteries. *Diam. Relat. Mater.* **2021**, *119*, 108553. [[CrossRef](#)]
97. Feng, D.; Li, Y.; Qin, X.; Zheng, L.; Guo, B.; Dai, W.; Song, N.; Liu, L.; Xu, Y.; Tang, Z.; et al. Biomass derived porous carbon anode materials for lithium-ion batteries with high electrochemical performance. *Int. J. Electrochem. Sci.* **2024**, *19*, 100488. [[CrossRef](#)]
98. Deng, W.N.; Li, Y.H.; Xu, D.F.; Zhou, W.; Xiang, K.X.; Chen, H. Three-dimensional hierarchically porous nitrogen-doped carbon from water hyacinth as selenium host for high-performance lithium–selenium batteries. *Rare Met.* **2022**, *41*, 3432–3445. [[CrossRef](#)]
99. Rahman, M.Z.; Edvinsson, T.; Kwong, P. Biochar for electrochemical applications. *Curr. Opin. Green Sustain. Chem.* **2020**, *23*, 25–30. [[CrossRef](#)]
100. Zeng, G.; Wang, Y.; Lou, X.; Chen, H.; Jiang, S.; Zhou, W. Vanadium oxide/carbonized chestnut needle composites as cathode materials for advanced aqueous zinc-ion batteries. *J. Energy Storage* **2024**, *77*, 109859. [[CrossRef](#)]
101. Li, Z.; Zhang, L.; Amirkhiz, B.S.; Tan, X.; Xu, Z.; Wang, H.; Olsen, B.C.; Holt, C.M.; Mitlin, D. Carbonized chicken eggshell membranes with 3D architectures as high-performance electrode materials for supercapacitors. *Adv. Energy Mater.* **2012**, *2*, 431–437. [[CrossRef](#)]

Disclaimer/Publisher's Note: The statements, opinions and data contained in all publications are solely those of the individual author(s) and contributor(s) and not of MDPI and/or the editor(s). MDPI and/or the editor(s) disclaim responsibility for any injury to people or property resulting from any ideas, methods, instructions or products referred to in the content.